

# Sensitivity analysis of dendritic growth kinetics in a Bridgman furnace front tracking model

R P Mooney<sup>a</sup>, S McFadden<sup>b</sup>

Trinity College Dublin, Dublin 2, Ireland.

Email: <sup>a</sup>rpmooney@tcd.ie, <sup>b</sup>shaun.mcfadden@tcd.ie

**Abstract.** A directional solidification experiment of a Ti–Al–Nb–B–C alloy by power down method is simulated using a Bridgman furnace front tracking model. The effect of varying the dendritic growth parameters;  $C$ , the columnar dendrite growth coefficient, and  $n$ , the undercooling exponent, is investigated. A matrix of growth coefficients and undercooling exponents - at three levels each, based around a growth law for Ti–46wt.%Al - is applied in simulations, and the effect on columnar dendrite tip temperature, tip velocity, and tip temperature gradient is observed. The simulation results show that the dendrite tip velocity and temperature gradient at the tip are practically unaffected by the use of different growth parameters. However, the predicted columnar dendrite tip undercooling did vary to give the required dendrite tip velocity. This finding has implications for the analysis of microstructural transitions, such as the Columnar to Equiaxed Transition (CET). In conclusion, it is suggested that, for transient solidification conditions, a CET prediction criterion based on tip undercooling is preferable to one that uses growth velocity.

## 1. Introduction

Many practical analytical models of dendritic growth use the Ivantsov parabolic model [1] to treat diffusion of heat and solute at the dendrite tip. Notable models include; marginal stability theory models based on the work Langer and Müller-Krumbhaar [2], such as the Lipton–Glicksman–Kurz (LGK) [3] model for equiaxed growth at small undercoolings, the Kurz–Giovanola–Trivedi (KGT) [4] model for columnar growth, and microsolubility theory models, as outlined by Kessler and Levine [5], where surface energy anisotropy is accounted for. In any such models, a velocity–undercooling relationship can be determined and it is possible to fit results to a power law curve so that the growth model can be more readily applied in subsequent numerical simulations. Rebow and Browne [6] demonstrated an example of this where the predicted growth velocity,  $V$ , was fitted to various levels of dendrite tip undercooling,  $\Delta T$ , by the power law;  $V=C\Delta T^n$ , where  $C$  (the growth coefficient) and  $n$  (the undercooling exponent) were the fitted variables for directional solidification of Al–4wt.%Cu and Al–2wt.%Si. In a similar way, the KGT model was used by Rebow et al. [7] to model columnar growth of Ti–46wt.%Al, where the stability parameter  $\sigma^*$  was set at 0.0506, i.e. twice the normal value used under the marginal stability criterion.

A Bridgman Furnace Front Tracking Model (BFFTM) [8] was recently applied to a thermal characterisation study [9] to determine the heat transfer coefficients of an experimental vertical Bridgman furnace. This characterisation study was a prerequisite for further experiments, which have since been carried out in the same furnace, investigating columnar to equiaxed transition (CET) in a multicomponent alloy of nominal composition; Ti–45.5Al–4.5Nb–0.2C–0.2B (at.%), using a power down method at four different cooling rates; 15 °C/min, 20 °C/min, 30 °C/min and 50 °C/min. Recently, Lapin et al. [10] reported on preliminary results from the experiment carried out at a cooling



rate of 30 °C/min (CET was observed in the sample processed at 30 °C/min only). The work reported on in this article and the work outlined in references [8], [9] and [10] has been carried out as part of the European Space Agency (ESA) backed research project: GRADECET (GRAvity DEpendance of Columnar to Equiaxed Transition in titanium alloys.)

The purpose of this article is to numerically model, using the BFFTM, the conditions at the columnar dendrite tip during the power down experiment carried out by Lapin et al. [10] at a cooling rate of 30 °C/min. The effect of varying the growth coefficient and undercooling index in the dendrite kinetic power law within the model - about central values taken from the Rebow model for TiAl - are simulated, observed and reported on. This *sensitivity analysis* of dendrite growth kinetics is important for this set of experimental data given that the current growth model is based on a binary alloy and therefore may include a margin of error.

There are several approaches to predicting CET given in the literature. A comparison of the alternative CET criteria is presented elsewhere [11]. The CET criterion used in this study is based on modelling columnar mush and comparing conditions at the columnar front on the Hunt [12] G-V diagram.

## 2. Method

### 2.1. Experimental method

The experimental method is described elsewhere in detail by Lapin et al. [10]. A schematic of the vertical Bridgman furnace used in the CET power down experiment is given in figure 1. The experimental procedure is summarised here as follows. Samples, 10 mm in diameter and 150 mm in length, were contained in a yttrium oxide crucible with wall thickness of 2.5 mm. The furnace chamber was flushed several times with high purity argon gas and back filled with argon to a pressure of 10 kPa (absolute). The experiment was carried out in three main stages. Firstly, in the heating and stabilization stage ( $t < 300$  s), the sample was heated until the fixed thermocouple reached 1720 °C where upon the sample was allowed to settle at this temperature for 300 s. Secondly, in the pulling stage ( $300 < t < 372$  s), the sample was drawn 20 mm into the crystalliser by the drive unit at a constant rate of 0.278 mm/s. Finally, in the power down stage ( $t > 372$  s), the heater temperature was reduced in a controlled manner so that the reference temperature, given by the fixed thermocouple, reduced at a rate of 30 °C/min.

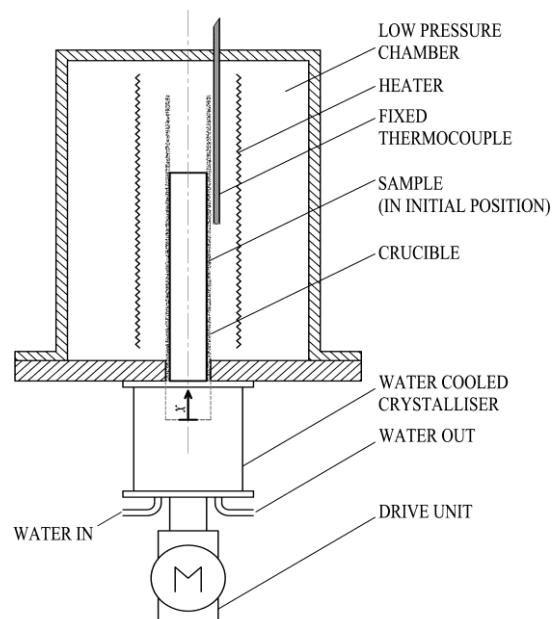


**Figure 1.** Schematic of the vertical Bridgman furnace apparatus.

## 2.2. Numerical method

The BFFTM [8] was used to model the experimental procedure. The modelled domain consisted of a series of disc-shaped control volumes (CVs) that contained the sample. Heat flow between CVs was permitted in the axial direction only. However, each CV had an individual radial heat flux component to account for heat gained (or lost) radially due to the proximity of the CV to the heater (or crystalliser). The BFFTM solves the following equation for heat flow in a rod (of cross-sectional area  $A$  and perimeter  $p$ ) moving at axial velocity  $u$ , using an explicit CV finite difference method,

$$\frac{\partial}{\partial t}(\rho c T) = \frac{\partial}{\partial x} \left( k \frac{\partial T}{\partial x} \right) - u \rho c \frac{\partial T}{\partial x} - \frac{hp}{A} (T - T_{\infty}) + E \quad , \quad (1)$$

where  $\rho$ ,  $c$  and  $k$  are the density, specific heat capacity and thermal conductivity of the alloy respectively,  $T_{\infty}$  and  $h$  are the temperature and heat transfer coefficient of the surrounding source (or sink), respectively, and  $E$  is the latent heat generated per unit volume. See reference [8] for a complete description of the numerical model. The results from a thermal characterisation study [9] were used to set the boundary conditions at either end of the domain and to set the heat transfer coefficients as a function of axial position in the furnace. Mooney et al. [9] gave a thorough account of the BFFTM algorithm as applied to this Bridgman apparatus using a similar TiAl multicomponent alloy. The BFFTM models columnar growth in the axial direction by tracking a front marker at the dendrite tips, thus providing information on the transient thermal conditions ahead of the columnar front. The information provided can then be used to determine the likelihood of a microstructural transition such as a CET. This method is an example of an indirect CET prediction method where the columnar mushy zone is simulated in the absence of an equiaxed mushy zone. The condition of the bulk undercooled liquid ahead of the columnar mushy zone is analysed with a view to predicting the likelihood of equiaxed nucleation and growth [11].

## 2.3. Growth kinetics matrix

A matrix of values for the growth coefficient  $C$ , and undercooling index  $n$ , were chosen to give a wide variation in growth rate versus undercooling based about central baseline values taken from the KGT columnar growth model power law fit for TiAl [7]. This range of values represents a  $\pm 38\%$  variation in  $C$  and a  $\pm 35\%$  variation for  $n$ , about the central values ( $C_2$  and  $n_2$ ) in Table 1.

**Table 1.** Matrix of values for growth coefficient and undercooling index.

| Growth coefficient,<br>$C$ [ $\text{m s}^{-1} \text{C}^{-n}$ ] | Undercooling index, $n$         |                                 |                              |
|--|---------------------------------|---------------------------------|------------------------------|
|  | $n_1 = 1.79$                    | $n_2 = 2.79$                    | $n_3 = 3.79$                 |
| $C_1 = 1.63 \times 10^{-6}$                                    | $n_1, C_1$ ..... (dotted green) | $n_2, C_1$ ----- (dashed green) | $n_3, C_1$ ——— (solid green) |
| $C_2 = 2.63 \times 10^{-6}$                                    | $n_1, C_2$ ..... (dotted red)   | $n_2, C_2$ ----- (dashed red)   | $n_3, C_2$ ——— (solid red)   |
| $C_3 = 3.63 \times 10^{-6}$                                    | $n_1, C_3$ ..... (dotted blue)  | $n_2, C_3$ ----- (dashed blue)  | $n_3, C_3$ ——— (solid blue)  |

Figure 2 shows the resulting set of velocity-undercooling curves when the power law ( $V=C\Delta T^n$ ) is applied using the values from Table 1. Lines of a specific colour (blue, red or green) share the same growth coefficient  $C$ , while lines of a specific type (solid, dashed or dotted) share the same the undercooling index  $n$ .

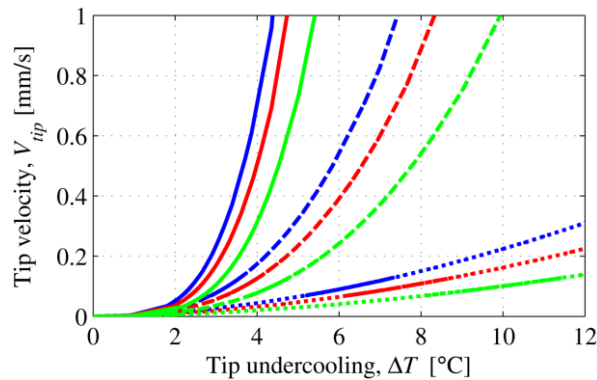


**Figure 2.** Columnar dendrite tip velocity versus dendrite tip undercooling for values of growth coefficient and undercooling index given in Table 1.

### 3. Results

Figure 3 shows (a) the simulated front position  $x$ , (b) the dendrite tip velocity  $V$ , and (c) the temperature gradient at the dendrite tip  $G$ , plotted against simulation time  $t$ , during the period:  $200 < t < 1200$  s. Figure 4 shows the simulated columnar dendrite tip velocity and temperature gradient at the dendrite tip plotted against columnar front position. Figure 5 shows the simulated dendrite tip temperature  $T_{tip}$ , and undercooling at the dendrite tip  $\Delta T$ , plotted against front position  $x$ . Figure 6 shows the columnar dendrite tip velocity plotted against the temperature gradient (similar to a Hunt [12] plot). In the analysis carried out by Lapin et al. [10] it was discovered that, for the sample cooled at  $30$  °C/min, the CET occurred at a position approximately  $76$  mm from the cold end of the sample. The point at which the front marker reaches this position in simulations is shown in figure 6.

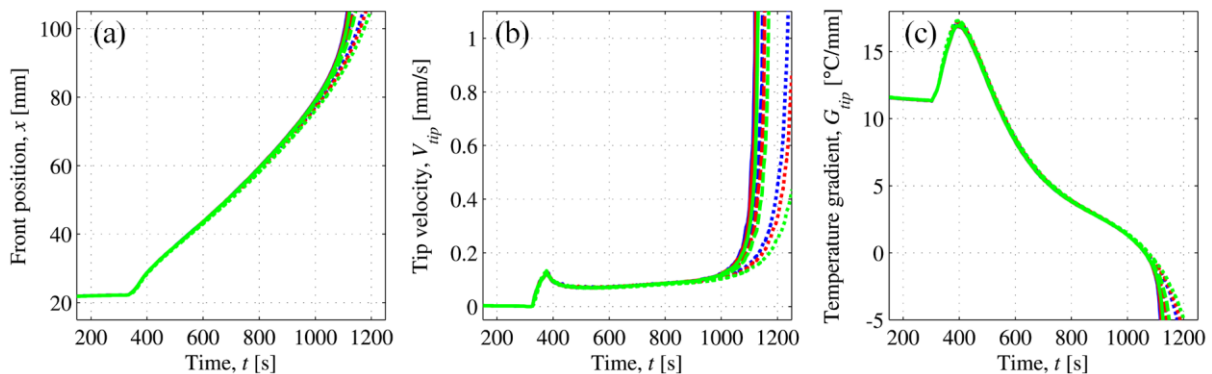


**Figure 3.** Simulated front position (a), columnar dendrite tip velocity (b) and temperature gradient at the dendrite tip (c) versus time.

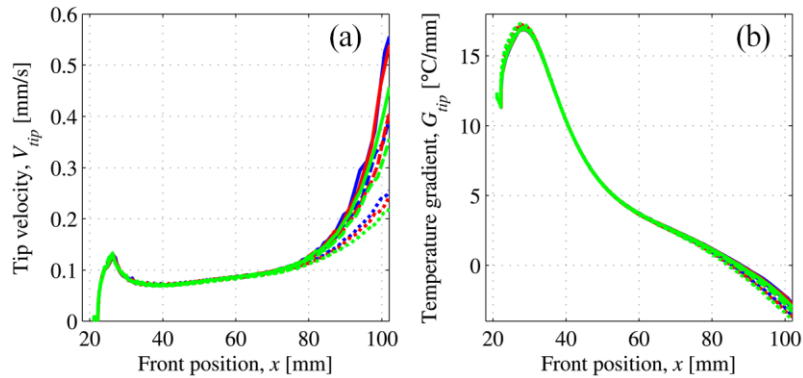


**Figure 4.** Simulated columnar dendrite tip velocity (a) and the temperature gradient at the dendrite tip (b) versus front position.

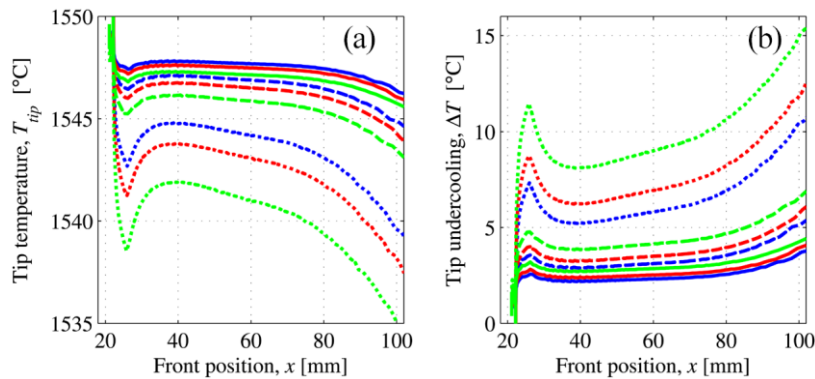


**Figure 5.** Simulated dendrite tip temperature (a) and undercooling at the dendrite tip (b) versus front position.

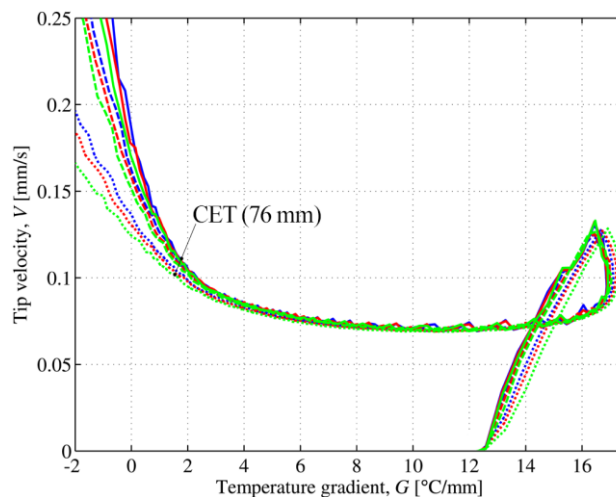


**Figure 6.** Columnar dendrite tip velocity versus temperature gradient at the dendrite tip.

#### 4. Discussion

In the results it is important to note the timings for the different stages of the experiment/simulation. In the initial heating and stabilization stage of the simulation ( $t < 300$  s) no movement or cooling of the sample occurs. This stage is of minimal interest for solidification because the system is stable.

Directional solidification begins when the pulling stage starts at time  $t = 300$  s. During this stage the sample is pulled into the water-cooled crystalliser at a fixed rate. At time  $t = 372$  s the pulling stage ends and the power down stage begins to cool the sample at a rate of  $30$  °C/min.

In all simulations it is important to note that the CET position measured by post mortem analysis in the experimental sample was  $76$  mm. Since we are modelling columnar growth only we can say that the simulation is only valid up to this position. According to the model predictions, the equivalent time for the columnar front at  $76$ mm is approximately  $975$  s regardless of the growth parameters used in the simulation.

In figure 3 (a) we see the temporal progress of the columnar front position for each pair of growth parameters in Table 1. It is clear that, for times up to approximately  $1000$  s, the simulated progress of the columnar front is practically unaffected by different growth parameters in the model. A similar outcome is observed in the simulated results for velocity curves plotted against time in figure 3 (b) and simulated temperature gradient plotted against time in figure 3 (c).

In figure 4 we see the tip velocity (a) and temperature gradient at the tip (b) plotted against columnar front position. As with results in figure 3 the model's results with different combinations of growth parameters displayed an indifference to tip velocity and temperature gradient up to and including the point where the CET occurred. This point is also well illustrated by the Hunt plot given in figure 6.

In figure 5 the temperature at the dendrite tip (a) and tip undercooling (b) are plotted against front position. In this case the lines are not overlapping and we see the true effect of varying the growth parameters in the dendrite growth law. The temperature at the dendrite tip, and consequently the tip undercooling, varies accordingly so that the power law;  $V = C\Delta T^n$ , delivers the growth velocity required to satisfy the cooling conditions imposed on the sample by the process. The simulated tip undercooling at CET, for the baseline set of growth parameters ( $n_2, C_2$ ), was  $3.8$  °C. The highest simulated tip undercooling at CET,  $\Delta T = 10.1$  °C, occurred using the lowest pair of growth parameters ( $n_1, C_1$ ), and conversely, the lowest simulated tip undercooling at CET,  $\Delta T = 2.5$  °C, occurred when using the highest pair of growth parameters ( $n_3, C_3$ ).

It is clear from references [8] and [9] that the BFFTM is appropriate for situations where the Biot number (the ratio of thermal resistance within the sample to the thermal resistance at its circumference) is less than  $0.1$ . The Biot number did not exceed  $0.03$  in all of the simulations discussed here. In this respect, an axial heat flow assumption is vindicated. The 1-dimensional heat flow assumption is not appropriate when the axial temperature gradient becomes comparable with the radial temperature gradient. This point is expanded upon in recent results published elsewhere [13].

## 5. Conclusion

A Front Tracking Model of transient directional solidification in a Bridgman furnace was developed. The model predicted the temperature evolution and growth conditions at the columnar front position, and it was deemed to be an appropriate model of the solidification process up to the point of CET only. A sensitivity study using the model showed that the predicted growth velocity and temperature gradient at the dendrite tip were insensitive to changes in the dendrite kinetics growth parameters. It is postulated that the operating conditions of the furnace (pulling rate and cooling rate) dictate the growth velocity (solidification rate) and temperature gradients. However, the simulated dendrite tip temperature and undercooling at the columnar dendrite tip were shown to be sensitive to the choice of dendrite growth parameters.

It is accepted in literature [11] that the condition of the bulk undercooled liquid ahead of the columnar front is important in predicting the onset of the equiaxed mushy zone and, hence, the CET. The extent of constitutional undercooling ahead of the columnar front is dependent on the tip undercooling and temperature gradient at the columnar front. Hence, accurate knowledge of the thermal conditions at the tip is required.

The results provided here demonstrate a particular shortcoming of the classic Hunt CET analysis [12] when applied to transient directional solidification. The Hunt analysis (developed for the steady-

state Bridgman scenario) considers the combination of  $G$  and  $V$  as the defining parameter set for predicting CET. We show that the  $G$ - $V$  plot is insensitive to the selection of dendrite growth parameters. Furthermore, we show that the undercooling at the tip (which is an indicator of conditions for CET), is sensitive to the selected dendrite growth parameters and deserves special attention.

In conclusion it is suggested that, for transient solidification conditions, a CET prediction criterion based on tip undercooling is preferable to one that uses velocity.

### Acknowledgments

This work was funded by European Space Agency PRODEX contract 4000107132 via Enterprise Ireland. The authors thank their GRADECET project partners: U. Hecht of ACCESS e.V. and Prof. J. Lapin of the Institute of Materials and Machine Mechanics at the Slovak Academy of Sciences.

### References

- [1] G P Ivantsov 1947 *Doklady Akademiyi Nauk SSSR* **58** 567
- [2] J S Langer and H Müller-Krumbhaar 1978 *Acta Metallurgica* **26** 11 1681–1687
- [3] J Lipton M E Glicksman and W Kurz 1987 *Metallurgical Transactions A* **18** 2 341–345
- [4] W Kurz B Giovanola and R Trivedi 1986 *Acta Metallurgica* **34** 5 823–830
- [5] D A Kessler and H Levine 1986 *Physical Review Letters* **57** 24 3069–3072
- [6] M Rebow and D J Browne 2007 *Scripta Materialia* **56** 6 481–484
- [7] M Rebow D J Browne and Y Fautrelle 2010 *Materials Science Forum* **649** 243–248
- [8] R P Mooney S McFadden M Rebow and D J Browne 2012 *Transactions of the Indian Institute of Metals* **65** 6 527–530
- [9] R P Mooney S McFadden Z Gabalcová and J Lapin 2014 *Applied Thermal Engineering* **67** 1–2 61–71
- [10] J Lapin Z Gabalcová U Hecht R P Mooney and S McFadden 2014 *Materials Science Forum* **790–791** 193–198
- [11] S McFadden D J Browne and C-A Gandin 2009 *Metallurgical and Materials Transactions A* **40** 3 662–672
- [12] J D Hunt 1984 *Materials Science and Engineering* **65** 1 75–83
- [13] R P Mooney U Hecht Z Gabalcová J Lapin and S McFadden 2015 *Kovove Materialy* **53** 3 187